Article ID: 1000-7032(2023)05-0921-11

Preparation and Application of Highly Fluorescent Purple-emissive Carbon Dots for Optical pH Measurement

WU Congying[1,2], ZHAO Xue[2], LIU Yuhui[1,2], HE Jingzong[1,2], LIU Shilin[1,2], WU Qilin[1,2*]

(1. *State Key Laboratory for Modification of Chemical Fibers and Polymer Materials, Donghua University, Shanghai* 201620, *China*;
2. *College of Materials Science and Engineering, Donghua University, Shanghai* 201620, *China*)

* *Corresponding Author, E-mail: wql@dhu. edu. cn*

Abstract: The preparation of purple-emissive carbon dots (P-CDs) usually accompanies the disadvantages of complicated preparation, low quantum yield (QY) and low fluorescence intensity. Herein, we used o-phenylenediamine (OPD) and m-phenylenediamine (MPD) as nitrogen sources and citric acid (CA) as carbon source to prepare P-CDs. Only using simple one-step hydrothermal method under a low experimental temperature of 120 ℃, we successfully obtained highly luminescent P-CDs with absolute QY of 5. 3%. The results of XPS and FT-IR revealed that all synthesized P-CDs contained similar functional groups but with different contents. The fluorescence intensity of P-CDs could be effectively regulated by the amount ratio of OPD to MPD. The resulting P-CDs also possessed considerable photostability and salt stability. Notably, the fluorescence color of P-CDs remarkably transformed into green as the pH being in the range of 1−3 or 10−13. The aforementioned unique pH-dependent fluorescence chromic behaviors ensured the potential application in the optical pH sensing.

Key words: high luminescence; purple-emissive carbon dots; optical pH sensing

CLC number: O482. 31 **Document code**: A **DOI**: 10. 37188/CJL. 20220330

高效紫色荧光碳点制备及光学 pH 检测应用

吴聪影[1,2], 赵 雪[2], 刘玉慧[1,2], 何敬宗[1,2], 柳仕林[1,2], 吴琪琳[1,2*]

(1. 东华大学 纤维材料改性国家重点实验室, 上海 201620;
2. 东华大学 材料科学与工程学院, 上海 201620)

摘要: 紫色荧光碳点(P-CDs)的制备通常存在制备复杂、量子产率低、荧光强度低等缺点。本文以邻苯二胺(OPD)和间苯二胺(MPD)为氮源,柠檬酸为碳源,在 120 ℃的低温条件下,通过一步水热法成功获得了绝对量子产率为 5.3% 的高荧光 P-CDs。XPS 和 FT-IR 结果表明,所有合成的 P-CDs 具有相似的官能团,但含量不同;OPD/MPD 的比例可有效调控 P-CDs 的荧光强度。所得 P-CDs 具有较好的光稳定性和盐稳定性。值得注意的是,当 pH 为 1~3 或 10~13 时,P-CDs 的荧光颜色明显转变为绿色。上述独特的 pH 依赖性荧光色行为确保了其在光学 pH 传感中的潜在应用。

关 键 词: 高荧光; 紫色荧光碳点; pH 光学检测

收稿日期: 2022-09-13; **修订日期**: 2022-10-08
基金项目: 国家自然科学基金重大项目(52090033/52090030)
Supported by National Natural Science Foundation of China(52090033/52090030)

1 Introduction

Carbon dots(CDs) are an emergent class of carbon-based fluorescent nanomaterials with outstanding properties of excellent electron donating/accepting abilities[1], biocompatibility[2], ecofriendly[3], chemical inertness, good water solubility and strong fluorescence[4-7]. During the past few decades, numerous researches have been carried out on various CDs for promising applications in fields of biomedicine[8-11], optoelectronics[12], sensing[13-14], photovoltaics[15], and electrocatalysis[16]. The CDs are mainly composed of carbon and oxygen elements, exhibiting a spherical state with a size range of 1−10 nm. They are predominantly amorphous with a sp^2 hybridized network of carbon[17].

In general, two main routes have been applied to prepare photoluminescent CDs, including top-down and bottom-up methods[18]. In the route of top-down, large carbon structures are exfoliated into small size CDs by chemical oxidation, laser ablation, electrochemical synthesis as well as arc-discharting. In these early stages, the CDs are usually prepared through the top-down method. Afterwards, these bottom-up techniques served as a new paradigm for advanced synthesis technique is slipping into the mainstream through the extensive concern and pioneering studies[19]. By contrast, bottom-up strategies are considered as the routes to obtain CDs by direct pyrolysis of small molecules[19]. Numerous bottom-up synthetic methods, including microwave-assisted synthesis, ultrasonic-assisted approach, hydrothermal treatment and thermal decomposition, have been developed[4]. Hydrothermal strategy, due to its low cost and easy manipulated parameters, is one of the most widespread methods to prepare CDs. However, compared to blue, yellow or green CDs, there is scarce research on the preparation and application of P-CDs. Even if there are reports that the preparation of P-CD is suffered from higher temperature or the use of organic reagents[20-21], leading to expensive costs and poor environmental protection for large scale application. Secondly, ultraviolet emission materials have an irreplaceable role in sterilization, anti-counterfeiting, biomedicine and other aspects[22]. However, since ultraviolet emission materials from noble gases and wideband gap semiconductors are expensive and rare, the potential application of P-CDs ultraviolet luminescence is of great value.

Furthermore, various doping methods have been applied to tune the fluorescent properties of CDs and deemed to be one of the most promising engineering methods to synthesize highly fluorescent CDs[23]. Owing to the similarly atomic size of nitrogen and carbon, nitrogen doping becomes the most commonly used strategy to regulate the properties of CDs. Although CDs with various colors fluoresce through doping or other strategies exhibit good photoluminescence(PL), P-CDs still have the disadvantages of low fluorescence intensity and low quantum yield(QY).

The pH value plays a critical role in both environmental and biological processes[24]. Since tight regulation of intracellular pH value is an important physiological function of organisms[25], achieving the visualization of such regulation will facilitate the understanding of physiological and pathological processes[26-27]. Therefore, various methods and techniques for intracellular pH sensing have been developed[28]. For example, Jin *et al*. demonstrated intracellular pH regulation inside living cells by using CDs as probes[29]. Plenty of CD probes have been widely used to monitor local pH values inside cells by measuring the increase or decrease in fluorescence intensity[30-32]. Generally, pH sensors are manufactured by CDs coated paper to meet the requirement of pH detection in the environment[33]. From above-mentioned, fluorescent CD probes have been established for the pH detection in environmental samples and *vivo/vitro* bioanalysis[4]. As far as we know, the fluorescence colors of CD probes can change with the switching of strong acidity and alkalinity of the environment.

In summary, in addition to the challenges of optimization of preparation conditions and improvement of optical properties, P-CDs are still faced with limited research as short-wavelength CDs, and it is urgent to expand the application of P-CDs. In this study, citric acid(CA) as a carbon source and two

anilines—o-phenylenediamine(OPD) and m-phenylenediamine(MPD) as nitrogen sources were adopted to synthesize P-CDs through a one-step hydrothermal method, as shown in Fig. 1. In addition, the effects of MPD concentrations on the fluorescence properties of P-CDs have been deeply investigated by changing the molar ratios of CA, OPD and MPD, which is expected to improve the fluorescence intensity and QY of P-CDs. Furthermore, we investigated the pH-dependent fluorescence chromic behaviors of P-CDs and proposed to use P-CDs as pH sensing probes.

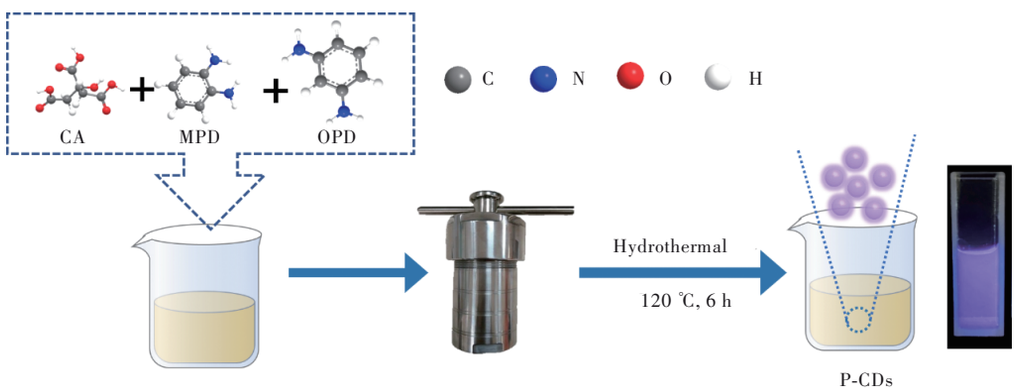

Fig.1　The synthesis route for P-CDs

2　Experiment

2.1　Synthesis of P-CDs

P-CDs were prepared by a hydrothermal method as depicted in Fig. 1. In particular, the molar ratio of CA, OPD and MPD was 0.67∶1∶1, and they were dissolved in 30 mL deionized water to form a clear solution (pH value maintained at 6 by using NaOH). The acquired solution (50 mL) was put into a Teflon-lined autoclave and then transferred to a homothermal oven at 120 ℃ for 6 h , and finally cooled to room temperature. To remove larger particles, the obtained solution was filtrated with ultra-filtration membrane (0.22 μm), and then dialysed through dialysis bag (500 u) for 48 h to obtained desired P-CDs aqueous solution. Subsequently, the P-CDs solution was kept in a freeze drier for 48 h to obtain solid P-CDs, which can be stored at room temperature.

P-CDs with different optical properties were synthesized under the same hydrothermal synthesis conditions by regulating the amounts of MPD(1−10 mol/L), but maintaining the constant concentration of CA(6.7 mol/L) and OPD(10 mol/L). The obtained P-CDs were defined as P-CDs*n* where *n* =1, 2, 3, 4, 5, 6, 7, 8, 9, 10 mol/L MPD.

2.2　Characterization

Transmission electron microscopy(TEM, JEM-2100, Japan) was used for analyzing the size and lattice structure of P-CDs. Flourier transform infrared spectrometer(FTIR, Nicolet6700, the United States) was applied to identify primary functional groups. Fluorescence spectra of CDs were recorded on an FL-2500 fluorescence spectrophotometer (FLS920, Edinburgh, Scotland). Absolute QY was measured by an integrating sphere (FLS920). A UV-3600 spectrophotometer (Tokyo, Japan) with a 1 cm path length cuvette was used to collected the UV Vis absorption spectrum. The X-ray photoelectron spectroscopy (XPS, Escalab250, the United States) of CDs were used to analyze the surface functional groups and element contents of CDs, and all results are based on a standard C1s peak with a binding energy calibration at 284.6 eV. The structural crystallinity of CDs was investigated by Powder X-ray diffraction (XRD; Bruker D8 Advance Diffractometer, the range of 2θ being 10°− 90°).

2.3　Optical pH Measurement

Experiments for the fluorescence detection of different pH were carried out in aqueous solution. The PL mechanism and pH-dependent fluorescence discoloration behaviors of P-CDs are shown in Fig. 2.

Firstly, P-CDs aqueous solution (1 mg/mL) was obtained by dissolving 0.01 g P-CDs in deionized water (10 mL). Afterward, the pH was adjusted to 1−13 by sodium hydroxide or hydrochloric acid aqueous solution. Different Fluorescence spectra were recorded at 380 nm excitation light.

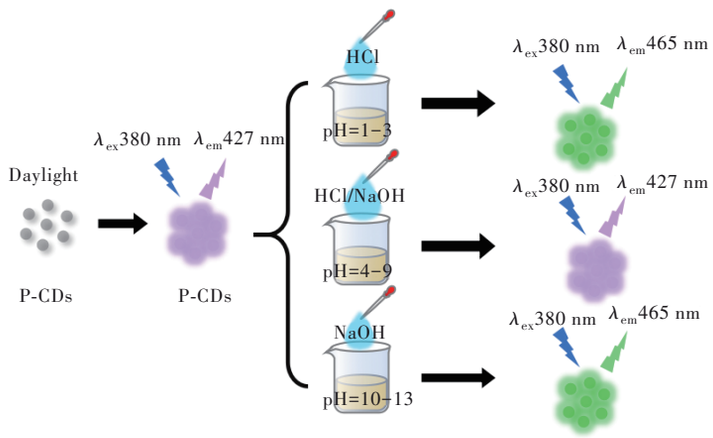

Fig.2 pH-dependent fluorescence chromic behaviors of P-CDs

3 Results and Discussion

3.1 Morphology and Structure Characterization

The morphological analysis of P-CDs was shown in Fig. 3(a). The P-CDs had a splendid dispersion with nearly similar sizes. The high resolution transmission electron microscopy (HRTEM) image (inset in Fig. 3(a)) implied that the clear lattice fringes of the P-CDs possess a lattice spacing of 0.278 nm, which was attributed to the (020) lattice plane of the P-CDs[34]. The dimension distributions of P-CDs were homogeneously illustrated in Fig. 3(b). Notably, the average particle size of the CDs was approximately 2.08 nm.

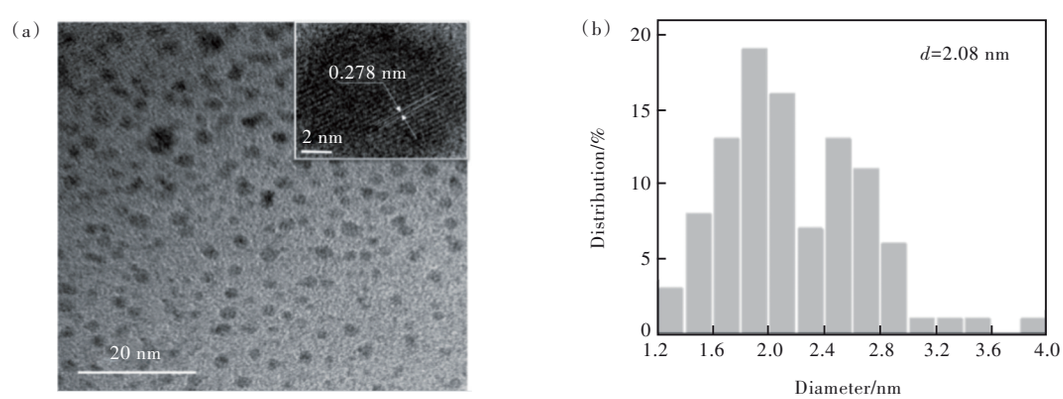

Fig.3 (a)TEM images and the lattice spacing of the P-CDs. (b)The size distribution was calculated from the TEM image in (a).

X-ray photoelectron spectra of P-CDs are shown in Fig. 4. The XPS survey spectrum in Fig. 4(a) indicated that the P-CDs comprised C(1s at 285 eV), O(1s at 531 eV), N(1s at 399 eV) elements with different contents of 64.08%, 28.18% and 7.74%, respectively. Furthermore, peak deconvolutions of the three elements were conducted to further interpret their nature. As displayed in Fig. 4(b), the high-resolution spectrum of C1s showed three main peaks at 284.78, 286.38, 288.18 eV which were corresponded to C=C(66%), C—O/C—N(2.18%) and C=O(31.83%), respectively. The results indicated that the P-CDs were mainly composed of C=C and were rich in C—O and C=O, which implied that P-CDs might have oxygen-rich functional groups based on the structure of the C=C. As shown in Fig. 4(c), the N1s demonstrated that three main peaks were at 398.77, 400.12, 401.21 eV, respectively, which meant that nitrogen atoms existed in the forms of pyrrole nitrogen, pyridine nitrogen and

graphite nitrogen as well. In addition, the spectrum of O1s (in Fig. 4(d)) can be divided into two peaks of 530.67 eV and 531.62 eV corresponding to C═O (30.56%) and C—O (69.44%), respectively. It can be inferred from the XPS results that the P-CDs comprised an aromatic polymer structure and were rich in oxygen-based groups such as the carboxyl, carbonyl, and hydroxyl groups.

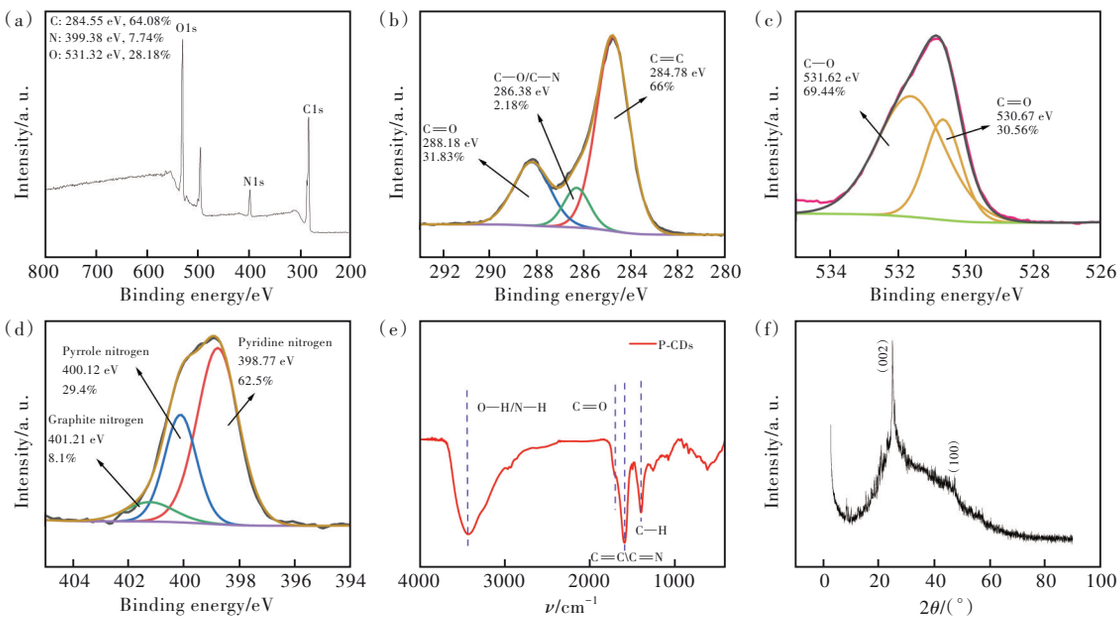

Fig.4　(a) Low range XPS spectra of P-CDs. High resolution de-convoluted XPS peaks for C1s(b), O1s(c) and N1s(d) of P-CDs. (e) FT-IR spectra of P-CDs. (f) XRD pattern of P-CDs.

The FT-IR spectrum was also detected, and the result was consistent with the XPS results. As shown in Fig. 4(e), the wide peak at 3 437 cm^{-1} was the stretching vibration of —OH or —NH, indicating the existence of hydroxyl or carboxyl groups and amino-groups in P-CDs. The sharp peak at 1 602 cm^{-1} was the telescopic vibration peak of C═C or C═N, indicating that there were numerous sp^2 structures that enriched the graphene in the P-CDs. These results were also consistent with those of TEM. In addition, the absorption peak at 1 261 cm^{-1} belonged to the stretching vibration of C—O—C. Fig. 4(f) showed the XRD pattern of P-CDs. It exhibited one strong peak and one weak peak at the range of 2θ=25° and 2θ=44°, that were assigned to (002) and (100) crystal planes of graphetic carbon, respectively, indicating the amorphous nature of CDs.

3.2　Optical Properties of P-CDs

The optical properties were discussed according to the UV-Vis and fluorescence spectra. The fluorescence absolute QY (η_{QY}) of P-CDs was calculated to be 5.30% according to η_{QY} equation as shown in Eq. (1):

$$\eta_{QY} = \frac{\int L_{emission}}{\int E_{solvent} - \int E_{sample}}, \qquad (1)$$

where η_{QY} is the absolute quantum yield, $L_{emission}$ is the number of fluorescent emission photons of the P-CDs, $E_{solvent}$ and E_{sample} are photon numbers of water and the excited by excitation light source, respectively.

According to the UV-Vis spectra shown in Fig. 5(a), the P-CDs had a wide absorption width between 230 nm and 350 nm. A sharp characteristic peak appeared at 237 nm induced by the graphite core of P-CDs, which is the typical optical characteristic of GQDs[35]. The absorbance peak at 237 nm was followed by a relatively but distinct peak at 280 nm. This can be attributed to the π-π^* transition of the conjugated C═C bond of graphitic carbon (sp^2 hybridized) present on the surface and the n-π^* transition of surface functional groups[36]. The absorbance within 310–400 nm range was broad and no obvious peaks could be identified after deconvolution.

According to that, the absorbance was not only decided by the specific chromophore, but probably related to multiple factors such as surface defects, presence of impurities and adsorbed molecules on the surface[37]. Further optical characteristics of the P-CDs are shown in Fig. 5(a). The optimal excitation wavelength of the P-CDs was 380 nm, and the emission wavelength was 427 nm, which was located in the purple region of the visible spectrum.

At different excitation wavelengths, the maximum emission wavelengths of P-CDs remained around 427 nm (Fig. 5(b)), which implied the P-CDs have good mono-chromaticity owing to the uniformity of size and surface states[38]. The constant emission wavelength also indicated that the P-CDs only contained a single emitter, which can avoid auto-fluorescence and be favorable for their application in quantitative assays. It can be also found that the P-CDs presented the highest fluorescent intensity when excited at 380 nm, thus 380 nm was selected as the excitation wavelength for the following experiments[33].

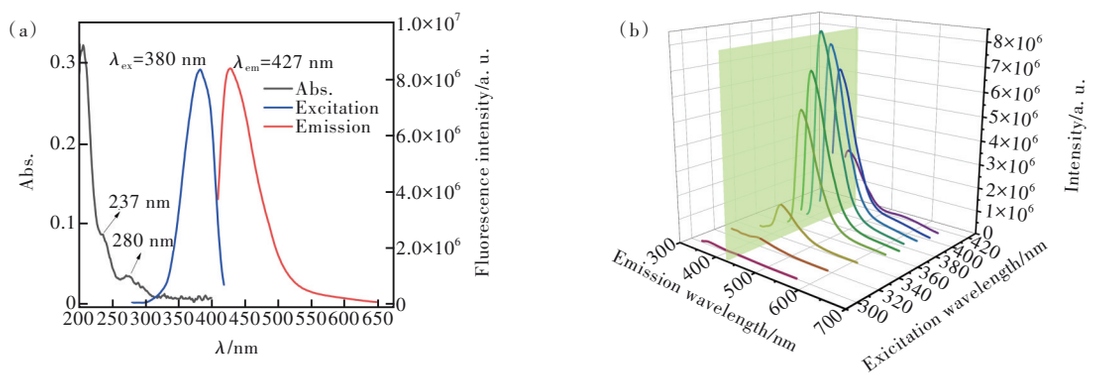

Fig.5 (a) UV-Vis absorption, excitation and emission spectra of the P-CDs. (b) Fluorescence spectra of P-CDs excited at different wavelengths.

The stability was of particular importance for nanomaterials. To obtain better performance, several detection conditions (such as UV irradiation time and NaCl concentration) were investigated. The fluorescence intensity of P-CDs slightly decreased with the excitation of UV irradiation time, but the fluorescence intensity was not affected by high concentration of NaCl solution (see Fig. S1), indicating that P-CDs have good photostability and salt stability.

3.3 Affecting Role of MPD on the Fluorescence Property

As shown in Fig. 6, the fluorescence property of P-CDs significantly changed with the increasing additive amounts of MPD. The fluorescence spectra showed an optimized excitation peaked at 380 nm, under which the maximum emission wavelength was observed around 427 nm (Fig. 6). It is interesting to find that the fluorescence intensity of P-CDs showed an overall upward trend with the addition of MPD, but there emerged a large fluctuation in case of MPD being 5 mol/L or 7 mol/L. This fluctuation may be related to sp^2/sp^3 carbon hybridization domain in the structure of P-CDs.

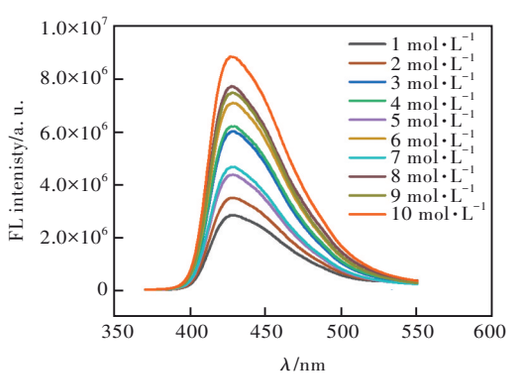

Fig.6 The Fluorescence spectra of P-CDs with different concentrations of MPD

In order to further reveal the relationship between the change of CDs properties and MPD additive amount, XPS characterization (Fig. S2) and FT-IR analysis (Fig. S3) were carried out for ten samples of P-CDs. The XPS spectra of all P-CDs showed three typical peaks: O1s (~531.72 eV), N1s (~399.38 eV) and C1s (~284.99 eV). FT-IR results showed that all P-CDs showed similar chemical

bonds and structures.

According to the proportion of atoms of different *C* species in XPS, the ratio of sp^2/sp^3 hybridization domain of ten P-CDs were calculated (see Tab. 1), and the relationship between fluorescence intensity of different P-CDs and sp^2/sp^3 hybridization domain was further explored. In cases of MPD being of 0–4 mol/L, the change of sp^2/sp^3 hybridization factor was opposite to the fluorescence intensity. Soon afterwards, fluorescence intensity and hybridization factor kept step with each other, as shown in Fig. 7.

Tab. 1　Elemental analysis of XPS determination and calculation of conjugate region

Samples	*C*/%			sp^2/%	sp^3/%	sp^2/sp^3
	C—C	C=C	C=O			
$P\text{-}CDs_1$	24.67	23.62	12.31	35.93	24.67	1.456
$P\text{-}CDs_2$	32.75	13.43	13.44	26.87	32.75	0.820
$P\text{-}CDs_3$	36.35	10.26	13.52	23.78	36.35	0.654
$P\text{-}CDs_4$	25.15	21.14	12.63	33.77	25.15	1.343
$P\text{-}CDs_5$	27.89	27.38	9.85	37.23	27.89	1.335
$P\text{-}CDs_6$	27.41	27.61	10.15	37.76	27.41	1.378
$P\text{-}CDs_7$	34.57	20.98	9.82	30.80	34.57	0.891
$P\text{-}CDs_8$	27.22	25.73	10.32	36.05	27.22	1.324
$P\text{-}CDs_9$	27.14	22.06	11.53	33.59	27.14	1.238
$P\text{-}CDs_{10}$	18.33	20.19	7.97	28.16	18.33	1.536

When the reaction raw materials were only OPD and CA, amidation reaction would occur (Fig. 8(a)). Low temperature may facilitate the formation of zigzag edge carbon net structure thereby

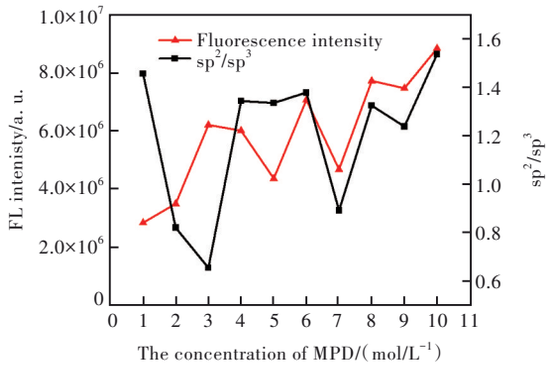

Fig.7　Comparison of fluorescence intensity and sp^2/sp^3 hybridization domain of different P-CDs

occurring sp^2C in-plane vibration, leading to the red shift of emission peak of CDs and easier formation of long wavelength CDs. With the addition of MPD, dehydration reaction may dominate this process and produce an armchair edge structure with sp^3C vibration (Fig. 8(b)), which could cause the blue shift of the emission peak of CDs and make the generated CDs emit purple fluorescence[39]. Therefore, as the amount of MPD increased, the fluorescence intensity of P-CDs would be enhanced. However, due to excessive aniline, the amino groups of OPD and MPD and carboxyl groups of CA would have competitive reactions. The contents of sp^2C and sp^3C would change and showed great fluctuations, but the fluorescence intensity of P-CDs generally presented an upward trend.

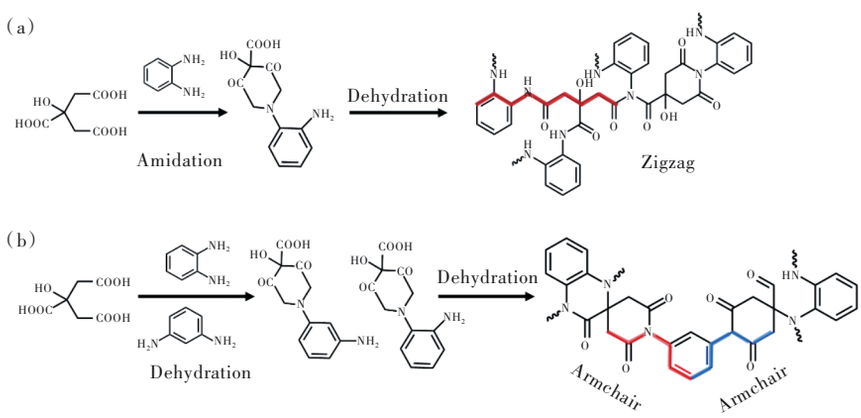

Fig.8　(a)OPD+CA reaction. (b)MPD+OPD+CA reaction.

3.4　pH Sensing

The fluorescence color of P-CDs was mutated in extreme acid and alkali environment. Therefore, the application of P-CDs in pH sensing was explored. We investigated the PL activities of P-CDs at different pH levels (pH=1–13). Fluorescence intensities with different pH are shown in Fig. 9(a) and (b). Interestingly, the obtained P-CDs exhibited particular pH-dependent fluorescence behaviors. At 380 nm excitation, the P-CDs exhibited two distinct colors *i.*

e. green fluorescent at strong acid(pH=1-3) or alkali solution (pH=10-13), but purple fluorescent at neutral solution(pH=4-9). The details of the three fluorescent zones were as follows.

Zone Ⅰ(pH=1-3): In extreme acid environment, the strong carboxyl protonation on the surface of P-CDs[40-41] will lead to the change of the existing form of functional groups on the surface of P-CDs and affect the surface defects, and finally resulting in the mutation of the fluorescence color of CDs to green (Fig. 9(d)). It was seen that with the decreasing pH changed from 3 to 1, emission intensity of CDs gradually reduced and higher concentration of H^+ (pH=1) intensity was quenched almost 97%. The surface carboxyl groups of CDs were protonated at lower pH level and aggregation of CDs occurred due to protonation of surface groups leading to fluorescence quenching. Therefore, the fluorescence intensity green emission of P-CDs was almost quenched at pH=1.

Zone Ⅱ(pH=4-9): The fluorescence intensity did not change obviously, showing pH independence in this zone.

Zone Ⅲ(pH=10-13): In extreme alkaline environment, deprotonation occurred on the surface of P-CDs, which changed the functional group states of CDs and made fluorescent CDs emit green light (Fig. 9(d))[42]. The CDs were stable in the pH range of 10 to 13, that is, the fluorescence intensity decreased only slightly with the increase of pH.

Because of the color mutation in the pH response process, P-CDs were proposed to be used in pH sensing. Therefore, the stability and repeatability of pH detection should be investigated. We have carried out this pH sensing experiments up to 5 repeat circulations by alternating pH at 2, 7 and 13, respectively. It can be seen that the P-CDs showed a remarkable pH-switching fluorescence property with no visible perturbation even after five cycles, implying the high pH-reversibility (Fig. 9(c)).

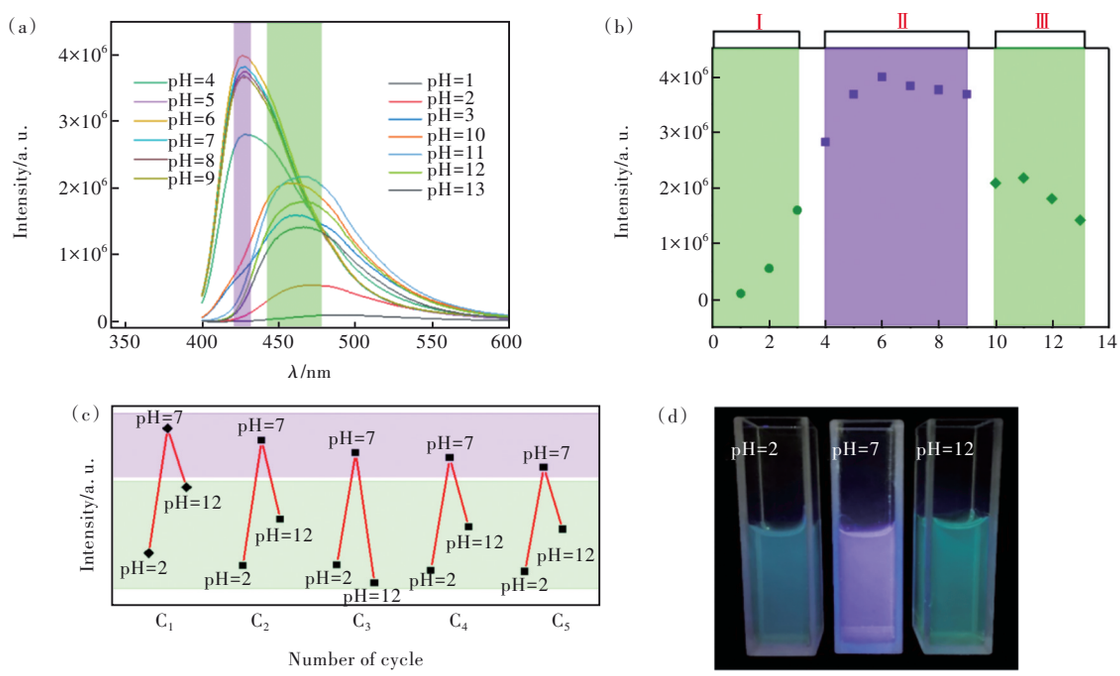

Fig.9 (a)The emission spectra of P-CDs at different pH. (b)The three fluorescent zones. (c)pH reversibility. (d)Colors of P-CDs aqueous solution under UV light.

Finally, this work was compared with some recently reported works. As displayed in Tab. 2, those CDs prepared by solvothermal methods(only using CA/OPD) mostly inclined to emit blue or green fluorescence[43]. Moreover, benefiting to the participation of MPD, this work decreased the reaction temperature from 240 ℃[20] to 120 ℃, only using water as the solvent.

Tab. 2　Comparison of CDs in literature and P-CDs in this paper

Precursors	Solvent	Temperature/℃	PL-peak/nm	Fluorescence color	QY	Applications	References
CA/OPD	Water	160	440	Blue	92.1%(A)	Bioimaging	[43]
CA/OPD	Water	240	413	Purple	—	LED	[20]
CA/OPD	Water	200	446	Blue	49%	Detection	[21]
CA/OPD	Water	200	432	Blue	83%	pH sensing	[44]
CA/OPD	DMF	180	515	Green	—	Detection	[45]
CA/OPD	Et	180	425	Blue	50.2%	Bioimaging	[46]
CA/MPD	Et	180	435	Blue	54.3%	Bioimaging	[46]
CA/OPD/MPD	Water	120	427	Purple	5.3%(A)	pH sensing	This work

4　Conclusions

In summary, using a simple one-pot hydrothermal method, P-CDs were successfully prepared from CA, OPD and MPD, avoiding strong acid/alkali conditions and high synthesis temperature. The resulting P-CDs demonstrated good water solubility, high fluorescence intensity, and good optical stability. The fluorescence intensity of P-CDs could be effectively regulated by adjusting the addition amount of MPD. With the increase of aniline, the competition between OPD and MPD was gradually strengthened, resulting in the changes of sp^2C/sp^3C in P-CDs structure, as well as the fluorescence intensity. The resultant P-CDs presented excellent discoloration performance under extreme acid/alkali environment. The significant fluorescence chromic properties coupled with high reversibility and repeatability guarantee the application of P-CDs in the fields of pH sensors in organisms.

Supplementary Information and Response Letter are available for this paper at: http://cjl.lightpublishing.cn/thesisDetails#10.37188/CJL.20220330.

References:

[1] LIU N, TANG M. Toxicity of different types of quantum dots to mammalian cells *in vitro*: an update review [J]. *J. Hazard. Mater.*, 2020, 399: 122606-1-15.

[2] MONDAL T K, MONDAL S, GHORAI U K, *et al.* White light emitting lanthanide based carbon quantum dots as toxic Cr (Ⅵ) and pH sensor [J]. *J. Colloid Interface Sci.*, 2019, 553: 177-185.

[3] PARK Y, YOO J, LIM B, *et al.* Improving the functionality of carbon nanodots: doping and surface functionalization [J]. *J. Mater. Chem.* A, 2016, 4(30): 11582-11603.

[4] KUMAR V B, PORAT Z, GEDANKEN A. Synthesis of doped/hybrid carbon dots and their biomedical application [J]. *Nanomaterials(Basel)*, 2022, 12(6): 898-1-27.

[5] HAN Z, LONG Y W, PAN S, *et al.* Efficient one-pot synthesis of carbon dots as a fluorescent probe for the selective and sensitive detection of rifampicin based on the inner filter effect [J]. *Anal. Methods*, 2018, 10(33): 4085-4093.

[6] ASHRAFIZADEH M, MOHAMMADINEJAD R, KAILASA S K, *et al.* Carbon dots as versatile nanoarchitectures for the treatment of neurological disorders and their theranostic applications: a review [J]. *Adv. Colloid Interface Sci.*, 2020, 278: 102123-1-12.

[7] DING H, ZHOU X X, WEI J S, *et al.* Carbon dots with red/near-infrared emissions and their intrinsic merits for biomedical applications [J]. *Carbon*, 2020, 167: 322-344.

[8] CUI F C, YE Y L, PING J F, *et al.* Carbon dots: current advances in pathogenic bacteria monitoring and prospect applications [J]. *Biosens. Bioelectron.*, 2020, 156: 112085-1-13.

[9] DÖRING A, USHAKOVA E, ROGACH A L. Chiral carbon dots: synthesis, optical properties, and emerging applications [J]. *Light Sci. Appl.*, 2022, 11(1): 75-1-23.

[10] WALTHER B K, DINU C Z, GULDI D M, *et al.* Nanobiosensing with graphene and carbon quantum dots: recent advances [J]. *Mater. Today*, 2020, 39: 23-46.

[11] LI M X, CHEN T, GOODING J J, *et al*. Review of carbon and graphene quantum dots for sensing [J]. *ACS Sens.*, 2019, 4(7): 1732-1748.

[12] ZHANG T Y, WANG X, WU Z Y, *et al*. Carbon dots promote the carrier recombination in Poly (9-vinyl carbazole) to enhance its electroluminescence [J]. *Appl. Surf. Sci.*, 2022, 585: 152649-1-9.

[13] NAIK V M, BHOSALE S V, KOLEKAR G B. A brief review on the synthesis, characterisation and analytical applications of nitrogen doped carbon dots [J]. *Anal. Methods*, 2022, 14(9): 877-891.

[14] MOLAEI M J. The optical properties and solar energy conversion applications of carbon quantum dots: a review [J]. *Solar Energy*, 2020, 196: 549-566.

[15] TIAN L, LI Z, WANG P, *et al*. Carbon quantum dots for advanced electrocatalysis [J]. *J. Energy Chem.*, 2021, 55: 279-294.

[16] MANIOUDAKIS J, VICTORIA F, THOMPSON C A, *et al*. Effects of nitrogen-doping on the photophysical properties of carbon dots [J]. *J. Mater. Chem.* C, 2019, 7(4): 853-862.

[17] WANG X, FENG Y Q, DONG P P, *et al*. A mini review on carbon quantum dots: preparation, properties, and electrocatalytic application [J]. *Front. Chem.*, 2019, 7: 671-1-9.

[18] SHEN C L, LOU Q, LIU K K, *et al*. Chemiluminescent carbon dots: synthesis, properties, and applications [J]. *Nano Today*, 2020, 35: 100954-1-23.

[19] HU S L, TRINCHI A, ATKIN P, *et al*. Tunable photoluminescence across the entire visible spectrum from carbon dots excited by white light [J]. *Angew. Chem. Int. Ed.*, 2015, 54(10): 2970-2974.

[20] WANG B Y, YU J K, SUI L Z, *et al*. Rational design of multi-color-emissive carbon dots in a single reaction system by hydrothermal [J]. *Adv. Sci.* (*Weinh.*), 2021, 8(1): 2001453-1-8.

[21] HAN Z, NAN D Y, YANG H, *et al*. Carbon quantum dots based ratiometric fluorescence probe for sensitive and selective detection of Cu^{2+} and glutathione [J]. *Sens. Actuators* B *Chem.*, 2019, 298: 126842-1-9.

[22] WANG X, ZHANG X Y, GU X Q, *et al*. A bright and stable violet carbon dot light-emitting diode [J]. *Adv. Opt. Mater.*, 2020, 8(15): 2000239-1-8.

[23] GUO Y M, WANG Z, SHAO H W, *et al*. Hydrothermal synthesis of highly fluorescent carbon nanoparticles from sodium citrate and their use for the detection of mercury ions [J]. *Carbon*, 2013, 52: 583-589.

[24] CHEN J, TANG Y, WANG H, *et al*. Design and fabrication of fluorescence resonance energy transfer-mediated fluorescent polymer nanoparticles for ratiometric sensing of lysosomal pH [J]. *J. Colloid Interface Sci.*, 2016, 484: 298-307.

[25] HAN J J, BURGESS K. Fluorescent indicators for intracellular pH [J]. *Chem. Rev.*, 2010, 110(5): 2709-2728.

[26] XING Y, ZHOU Y, FAN L, *et al*. Construction strategy for ratiometric fluorescent probe based on Janus silica nanoparticles as a platform toward intracellular pH detection [J]. *Talanta*, 2019, 205: 120021-1-7.

[27] WANG N N, YU X Y, DENG T, *et al*. Two-photon excitation/red emission, ratiometric fluorescent nanoprobe for intracellular pH imaging [J]. *Anal. Chem.*, 2020, 92(1): 583-587.

[28] JIN X Z, SUN X B, CHEN G, *et al*. pH-sensitive carbon dots for the visualization of regulation of intracellular pH inside living pathogenic fungal cells [J]. *Carbon*, 2015, 81: 388-395.

[29] SHANGGUAN J F, HE D G, HE X X, *et al*. Label-free carbon-dots-based ratiometric fluorescence pH nanoprobes for intracellular pH sensing [J]. *Anal. Chem.*, 2016, 88(15): 7837-7843.

[30] WANG X Y, WANG Y S, PAN W, *et al*. Carbon-dot-based probe designed to detect intracellular pH in fungal cells for building its relationship with intracellular polysaccharide [J]. *ACS Sustainable Chem. Eng.*, 2021, 9(10): 3718-3726.

[31] QIN J, GAO X, CHEN Q Q, *et al*. pH sensing and bioimaging using green synthesized carbon dots from black fungus [J]. *RSC Adv.*, 2021, 11(50): 31791-31794.

[32] WANG R X, WANG X F, SUN Y M. One-step synthesis of self-doped carbon dots with highly photoluminescence as multifunctional biosensors for detection of iron ions and pH [J]. *Sens. Actuaors* B *Chem.*, 2017, 241: 73-79.

[33] CAYUELA A, SORIANO M L, CARRILLO-CARRIÓN C, *et al*. Semiconductor and carbon-based fluorescent nanodots: the need for consistency [J]. *Chem. Commun.*, 2016, 52(7): 1311-1326.

[34] TIAN X T, YIN X B. Carbon dots, unconventional preparation strategies, and applications beyond photoluminescence [J]. *Small*, 2019, 15(48): 1901803-1-30.

[35] DE B, KARAK N. A green and facile approach for the synthesis of water soluble fluorescent carbon dots from banana

juice [J]. *RSC Adv.*, 2013, 3(22): 8286-8290.

[36] GHOSH DASTIDAR D, MUKHERJEE P, GHOSH D, *et al.* Carbon quantum dots prepared from onion extract as fluorescence turn-on probes for selective estimation of Zn^{2+} in blood plasma [J]. *Colloids Surf.* A *Physicochem. Eng. Asp.*, 2021, 611: 125781-1-10.

[37] YU J K, YONG X, TANG Z Y, *et al.* Theoretical understanding of structure-property relationships in luminescence of carbon dots [J]. *J. Phys. Chem. Lett.*, 2021, 12(32): 7671-7687.

[38] SHEN L, HOU C J, LI J W, *et al.* A one-step synthesis of novel high pH-sensitive nitrogen-doped yellow fluorescent carbon dots and their detection application in living cells [J]. *Anal. Methods*, 2019, 11(44): 5711-5717.

[39] XU J H, LIANG Q L, LI Z J, *et al.* Rational synthesis of solid-state ultraviolet B emitting carbon dots *via* acetic acid-promoted fractions of sp^3 bonding strategy [J]. *Adv. Mater.*, 2022, 34(17): 2200011-1-8.

[40] XU J Y, SUN L L, GUO X J, *et al.* pH and solvent induced discoloration behavior of multicolor fluorescent carbon dots [J]. *Colloids Surf.* A *Physicochem. Eng. Asp.*, 2022, 648: 129261-1-8.

[41] LIU X X, YANG C L, ZHENG B Z, *et al.* Green anhydrous synthesis of hydrophilic carbon dots on large-scale and their application for broad fluorescent pH sensing [J]. *Sens. Actuators* B *Chem.*, 2018, 255: 572-579.

[42] MEIERHOFER F, DISSINGER F, WEIGERT F, *et al.* Citric acid based carbon dots with amine type stabilizers: pH-specific luminescence and quantum yield characteristics [J]. *J. Phys. Chem.* C, 2020, 124(16): 8894-8904.

[43] TAN A Z, YANG G H, WAN X J. Ultra-high quantum yield nitrogen-doped carbon quantum dots and their versatile application in fluorescence sensing, bioimaging and anti-counterfeiting [J]. *Spectrochim. Acta Part* A *Mol. Biomol. Spectrosc.*, 2021, 253: 119583-1-9.

[44] ZHAO X H, LI J, LIU D N, *et al.* Self-enhanced carbonized polymer dots for selective visualization of lysosomes and real-time apoptosis monitoring [J]. *iScience*, 2020, 23(4): 100982-1-24.

[45] 潘鹏涛, 邹凡雨, 殷俊磊. 碳纳米点荧光探针对有机溶剂中水含量的检测 [J]. 激光与光电子学进展, 2020, 57(23): 231602-1-6.
PAN P T, ZOU F Y, YIN J L. Carbon-nanodots as fluorescent probe for detection of water content in organic solvents [J]. *Laser Optoelectron. Progr.*, 2020, 57(23): 231602-1-6. (in Chinese)

[46] 姜杰, 李士浩, 严一楠, 等. 氮掺杂高量子产率荧光碳点的制备及其体外生物成像研究 [J]. 发光学报, 2017, 38(12): 1567-1574.
JIANG J, LI S H, YAN Y N, *et al.* Preparation of n-doped fluorescent carbon dots with high quantum yield for *in-vitro* bioimaging [J]. *Chin. J. Lumin.*, 2017, 38(12): 1567-1574. (in Chinese)

吴聪影(1998-),女,安徽亳州人,硕士,2023 年于东华大学获得硕士学位,主要从事碳点制备及应用的研究。
E-mail: 2200476@mail. dhu. edu. cn

吴琪琳(1970-),女,安徽黄山人,博士,教授,博士生导师,2002 年于东华大学获得博士学位,主要从事新型碳材料及其复合材料的研究。
E-mail: wql@dhu. edu. cn